Power production and microbial community composition in thermophilic acetate-fed up-flow and flow-through microbial fuel cells

Paolo Dessì [a,b,*], *Pritha Chatterjee* [a,c], *Simon Mills*[d], *Marika Kokko*[a], *Aino-Maija Lakaniemi* [a], *Gavin Collins*[d], *Piet N. L. Lens*[a,b]

[a]*Tampere University, Faculty of Engineering and Natural Sciences, P.O. Box 541, FI- 33104 Tampere University, Finland*

[b]*National University of Ireland Galway, University Road, Galway, H91 TK33, Ireland*

[c]*Department of Civil Engineering, Indian Institute of Technology Hyderabad, India*

[d]*Microbial Communities Laboratory, School of Natural Sciences, National University of Ireland Galway, University Road, Galway, H91 TK33, Ireland*

*****Corresponding author: Paolo Dessì, National University of Ireland Galway, University Road, Galway, H91 TK33, Ireland, phone: +353 830678774, e-mail: paolo.dessi@nuigalway.ie

Abstract

The microbial communities developed from a mixed-species culture in up-flow and flow-through configurations of thermophilic (55°C) microbial fuel cells (MFCs), and their power production from acetate, were investigated. The up-flow MFC was operated for 202 days, obtaining an average power density of 0.13 W/m^3, and *Tepidiphilus* sp. was the dominant transcriptionally-active microorganisms. The planktonic community developed in the up-flow MFC was used to inoculate a flow-through MFC resulting in the proliferation of *Ureibacillus* sp., whose relative abundance increased from 1 to 61% after 45 days. Despite the differences between the up-flow and flow-through MFCs, including the anode electrode, hydrodynamic conditions, and the predominant microorganism, similar (p=0.05) volumetric power (0.11-0.13 W/m^3), coulombic efficiency (16-18%) and acetate consumption rates (55-69 mg/L/d) were obtained from both. This suggests that though MFC design can shape the active component of the thermophilic microbial community, the consortia are resilient and can maintain similar performance in different MFC configurations.

Keywords

Attached community; Bioelectrochemical system; Electrogenic microorganisms; MFC; Planktonic community

1. Introduction

Microbial fuel cells (MFCs) enable electrical energy recovery from organic and inorganic compounds by coupling a biological oxidative reaction at the anode to a biotic, or abiotic, reductive reaction at the cathode (Logan et al., 2006). MFCs rely on electroactive microorganisms that use a solid anode electrode as electron acceptor for the oxidation of organic and inorganic substrates. The electron transfer to the anode electrode can be direct, *via* membrane-bound proteins or conductive nanowires, or indirect, *via* autogenous or heterogeneous mediators (Kumar et al., 2017). In particular, formation of an electroactive biofilm around the anode electrode was individuated as a key factor for efficient electricity production in MFCs (Kumar et al., 2017; Yang et al., 2019).

Most known electroactive microorganisms are mesophiles (Dattatraya Saratale et al., 2017), growing best somewhere in the range of 25-40°C. However, MFC operation at higher temperatures confers several advantages, such as fast microbial growth and reaction kinetics, high substrate solubility and mass transfer, low oxygen solubility, and significantly reduced contamination by competitive and pathogenic microorganisms (Dopson et al., 2016; Sekar et al., 2017). Indeed, thermophilic MFCs can be particularly suited for treatment of high-temperature waste streams – due to the much reduced energy requirement to heat the bioreactors – as well as of complex substrates and pathogenic streams (Shrestha et al., 2018).

However, thermophilic microbial communities typically harbour much less diversity than mesophilic consortia and, so, are considered less resilient and more vulnerable to potential process disturbances (Carballa et al., 2011). Further development, and application, of thermophilic MFCs is also hindered by a severe lack of information on thermophilic electroactive microbial communities. To date, only a few bacterial genera e.g., *Caloramator* (Fu et al., 2013a), *Thermincola* (Marshall and May, 2009; Parameswaran et al., 2013; Wrighton et al., 2008) and *Thermoanaerobacter* (Lusk

et al., 2015) from the Phylum Firmicutes, along with *Pyrococcus* (Sekar et al., 2017) (the Euryarchaeota) and *Calditerrivibrio* (Fu et al., 2013b) (the Deferribacteres), were reported as electricity producing at temperatures above 50℃ without addition of any mediators. Among them, direct electron transfer to the anode was demonstrated only with *Thermincola potens* (Wrighton et al., 2011), *Thermincola ferriacetica* (Parameswaran et al., 2013) and *Pyrococcus furiosus* (Sekar et al., 2017). Although MFCs were operated at temperatures up to even 98°C (Fu et al., 2015), most studies were conducted at 55-60°C. Firmicutes, Deferribacteres and Coprothermobacterota were the dominant bacterial phyla enriched from mixed cultures at 55-60°C in MFC anodes using acetate (Fu et al., 2013a; Jong et al., 2006; Mathis et al., 2008; Wrighton et al., 2008) or distillery wastewater (Ha et al., 2012) as substrate.

H-type MFC designs were most frequently used for studies of thermophilic MFCs inoculated with mixed-species cultures (Fu et al., 2015; Ha et al., 2012; Jong et al., 2006; Wrighton et al., 2008). A few exceptions include a sediment MFC operated at 60℃ (Mathis et al., 2008), as well as a MFC designed to control evaporation (which is a major operating challenge for thermophilic MFCs) (Carver et al., 2011). Efficient and easily scalable configurations, such as up-flow and flow-through MFCs, were proposed for mesophilic MFCs (Lay et al., 2015; ter Heijne et al., 2008), but have not yet been applied under thermophilic conditions. The shear forces produced by the different hydrodynamic conditions employed by various MFC configurations may affect the structure, and activity, of microbial communities underpinning the MFCs, as well as affecting the mass transfer, i.e. the exchange of substrate and products between the anolyte and the anode biofilm, which could, in turn, impact on power output (Cecconet et al., 2018). Thus, studies comparatively evaluating various MFC configurations for thermophilic electrogenesis, from both engineering and microbiological points of view, are now required.

New insights to thermophilic microbial consortia, and to community adaptation to different MFC configurations, would promote innovation in thermophilic MFC application. The toolbox of molecular microbial ecology provides various means to unravel complex communities, by analysing genetic markers and elucidating diversity, community structure, and even activity. DNA sequences provide information on phylogenetic diversity and community composition whilst RNA-level analyses help identify the active – or, at least, transcriptionally-active – subpopulation (Dessì et al., 2018).

The aim of this study was to characterise, for the first time, the anode-attached, and planktonic, microbial communities in, and compare the power generation by, acetate-fed, up-flow and flow-through MFCs configurations operated at 55°C.

2. Materials and methods

2.1 Up-flow MFC set-up

The up-flow MFC used in this study was first described by Lay et al. (2015). It consisted of a 500 mL anodic chamber and a 250 mL cathodic chamber separated by an anion exchange membrane (AEM AMI-7001, Membranes International Inc., USA) with a diameter of 4 cm (12.5 cm^2 area). The anode, previously described by Haavisto et al. (2019), was a steel cage (10×4×0.5 cm) containing approximately 15 g activated carbon granules (< 2 mm, Alfa Aesar). The cathode was a carbon plate (5×3×0.5 cm). The two electrodes were connected through a 100 Ω resistor using Ti wires. A reference electrode (Ag/AgCl SENTEK QM710X in 3 M KCl solution) was connected to the recirculation tube of the anode through a capillary glass tube (QiS, the Netherlands). The MFC was maintained at 55±1°C using heating coils. The anolyte was recirculated with a flow rate of 60 mL/min using a peristaltic pump (Masterflex®, USA). To ensure anaerobic conditions, the anodic chamber of the MFC was connected to a gas bag containing N_2.

2.2 Flow-through MFC set-up

The flow-through MFC set-up used was as previously described by Sulonen et al. (2015). It comprised of anodic and cathodic chambers (30 mL volume each) separated by an AEM (AMI-7001). Carbon plates, covered with carbon paper (Coidan graphite products, USA), were used as anode and cathode connected with a 100 Ω resistor. The effective area of both electrodes and the membrane was 22 cm^2. An Ag/AgCl reference electrode (BASi RE-5B) was inserted in the anodic chamber through a port, close to the anode electrode. A gas bag containing N_2 was connected to the other port of the anodic chamber. The flow-through MFC was operated inside a 55±1°C incubator (Melag Germany). Serum bottles placed in a water bath (VWR, USA) were used to recirculate anolyte and catholyte to the flow-through MFC at a flow rate of 60 mL/min using peristaltic pumps (Masterflex®, USA). The overall anodic and cathodic chamber volumes were similar to those of the up-flow MFC (500 and 250 mL, respectively). The temperature of the water bath was set to 65°C to compensate for heat loss from the tubes connecting the serum bottles to the flow-through MFCs in the incubator.

2.3 Composition of synthetic anolyte and catholyte

The synthetic anolyte of both the up-flow and flow-through MFCs was similar to that used by Mäkinen et al. (2012), but omitting EDTA and resazurin, and containing 1 g/L acetate (as 1.39 g/L sodium acetate) as carbon source, if not otherwise mentioned. The pH of the medium was adjusted to 7.0±0.1 with 5 M NaOH and flushed with N_2 for 5 min before delivery (500 mL) to the MFCs. The conductivity of the medium was 14-15 mS/cm. The catholyte of both MFCs was 200 mL potassium ferricyanide (50 mM) in 100 mM phosphate buffer (Haavisto et al., 2017).

149 *2.4 Up-flow MFC inoculation and operation*

150 The up-flow MFC was inoculated with a mixture (1 g volatile solids (VS) each) of sewage sludge
151 digestate (88 g total solids (TS)/L and 32 gVS/L) from a thermophilic (55°C) biogas plant
152 (Topinoja, Turku, Finland) and mature compost (0.56 gTS/g and 0.43 gVS/g) from a municipal
153 waste treatment facility (Tarastenjärvi, Tampere, Finland). 2-bromoethanesulphonic acid (BESA)
154 was added to the anolyte in the first feeding cycle at a concentration of 1 g/L to inhibit
155 methanogenic archaea, previously found as part of the active thermophilic (55°C) microbial
156 community in a xylose-fed, H-type MFC (Dessì et al., 2018). A potential of -287 mV *vs*. Ag/AgCl
157 (-60 mV *vs*. SHE at 55°C), previously shown to sustain the growth of the thermophilic electroactive
158 *Thermincola* sp. (Parameswaran et al., 2013), was imposed to the anode for 14 d using a
159 potentiostat (BioLogic VMP3, France). Then, the potentiostat was disconnected (day 0) and the up-
160 flow MFC was operated for 202 days with the two electrodes connected through a 100 Ω resistor.
161 The initial acetate concentration was 0.5 g/L, but was increased to 1.0 g/L after the first two feeding
162 cycles (day 19). The feeding steps were performed when > 60% acetate was consumed, by
163 replacing 100 mL (20%) of the anolyte with a fresh solution containing 5 g/L acetate, resulting in an
164 acetate concentration of 1.0-1.5 g/L in the anolyte. On the same days, the catholyte was replaced
165 with 200 mL of fresh ferricyanide solution. The catholyte was also replaced on days 15, 25, 34, 40,
166 86 and 137 when reduced power production was observed. On day 109, 100% of the anolyte was
167 replaced with the fresh solution, containing 1 g/L acetate, to evaluate possible changes in power
168 production due to flush-out of planktonic cells and mediators. The AEM was changed to a fresh one
169 on days 34 and 86.

170

171 *2.5 Flow-through MFC inoculation and operation*

172 The flow-through MFC was inoculated with 10 mL of anolyte (2.3 gVS/L) collected from the up-
173 flow MFC after 159 days operation and operated for 45 days. The feeding steps were performed by

174 replacing 100 mL (20%) of the anolyte with fresh anodic solution containing 5 g/L acetate, and
175 replacing 100% of catholyte on the same day. Fresh catholyte was also provided on days 21 and 28.
176
177 *2.6 Chemical and bioelectrochemical analyses*
178 Cell voltage and anodic and cathodic potentials (against the Ag/AgCl reference electrode) were
179 measured at intervals of 2 min using a data logger (Agilent 34970A, Agilent technologies, Canada).
180 Conductivity and pH were measured in liquid samples using a conductivity meter (Horiba
181 LAQUAtwin, Japan) and a pH meter (WTW pH 330 meter with Hamilton Slimtrode probe),
182 respectively. TS and VS were measured according to the APHA standard (APHA, 1998). Acetate
183 was measured using a gas chromatograph equipped with a flame ionisation detector (GC-FID) as
184 described by Haavisto et al. (2017). Polarisation analysis was conducted on day 45 and on day 17
185 for the up-flow and flow-through MFC, respectively, two days after the acetate feeding and
186 catholyte replacement, as described previously (Dessì et al., 2018).
187
188 *2.7 Calculations*
189 Current and power densities were calculated according to Logan et al. (2006) and normalised either
190 to the anolyte volume (0.5 L) or the effective anode electrode area (94.0 and 22.0 cm^2 for the up-
191 flow and flow-through MFC, respectively). All potentials are reported against the Ag/AgCl
192 reference electrode. The internal resistance was estimated from the slope of the polarisation curve.
193 The Coulombic efficiency (CE) was calculated based on the acetate removed, counting 8 mol
194 electrons exchanged per mol acetate consumed, according to the following equation (Logan et al.,
195 2006):
196
197 $2\ HCO_3^- + 9\ H^+ + 8\ e^- \rightarrow CH_3COO^- + 4\ H_2O$ (1)
198

199 Average current and power densities, and CE, were calculated based on the whole batch cycle.
200 Acetate consumption rates (A_{CR}) were calculated according to the following equation:
201
202 $$A_{CR} = (C_{Ai}-C_{Af})/t \quad (2)$$
203 where C_{Ai} and C_{Af} is the acetate concentration at the beginning and at the end of the batch cycle,
204 respectively, and t is the duration of the batch cycle.
205
206 One-way analysis of variance (ANOVA) at p=0.05 was conducted using the IBM SPSS program
207 (v24).
208
209 *2.8 Microbial community analysis*
210 Triplicate microbiological samples were collected at the end of the experiment from the biofilm-
211 containing activated carbon granules and the anolyte of the up-flow MFC, as well as from the
212 carbon paper electrode and the anolyte of the flow-through MFC. Anolyte samples were pelleted by
213 centrifugation (5 min, 5000 rpm) and pellets were re-suspended in 1 mL autoclaved 0.9% NaCl
214 solution, whereas activated carbon and carbon paper samples, cut in small pieces with sterile
215 scissors, were washed with, and then stored in, 0.9% NaCl. Extraction of total genomic DNA and
216 RNA was done using a modified version of the method from Griffiths et al. (Dessì et al., 2018;
217 Griffiths et al., 2000). cDNA synthesis from RNA was achieved as described previously (Dessì et
218 al., 2018). 16S rRNA gene sequences (from DNA and cDNA) were amplified using the primer pair
219 515F and 806R (Caporaso et al., 2011), and then used in high-throughput DNA sequencing using an
220 Illumina Miseq platform (FISABIO, Valencia, Spain). Due to insufficient biofilm formation – and,
221 thus, poor recovery of nucleic acids – only one of the triplicate samples from the carbon paper
222 electrode of the flow-through MFC could be used for sequencing; thus, that sample was excluded
223 from subsequent statistical analyses.

Bioinformatic processing of raw FASTQ sequence files was done using the Mothur pipeline (Schloss et al., 2009). Statistical analysis was carried out using R (Version 3.4.4) based on the data generated from the Mothur pipeline and on associated metadata. Alpha, and beta, diversity analyses were done using the vegan package (Oksanen et al., 2015). Alpha diversity analysis included (i) rarefied richness, (ii) Shannon entropy, and (iii) Pielou's evenness. Vegan's aov() function was used to calculate pair-wise ANOVA p-values, as indicated on alpha diversity plots. Non-Metric Multidimensional Scaling (NMDS) plots were constructed at the genus level using the Bray-Curtis distance metric and ellipses were drawn to represent a 95% confidence interval of the ordination point standard errors. Permutational analysis of variance (PERMANOVA) was done using the Vegan Adonis function.

3. Results and discussion

3.1 Power production from acetate in the up-flow MFC

Acetate was successfully converted to electricity during the 202 days of up-flow MFC operation. Power production increased in the first three feeding cycles, reaching an average of 0.2 W/m^3 in the third cycle (day 19) and suggesting the growth of the thermophilic electroactive community – as confirmed by falling anode potential from 0.1 to 0.04 V. This was also supported by the increasing rate of acetate consumption, which was 40.7 and 81.6 mg/L/d in the first and third feeding cycle, respectively. Over the subsequent 12 feeding cycles, the MFC produced an average power of 0.13 ± 0.04 W/m^3 (8.4 ± 2.2 mW/m^2). Higher power output of 150-300 mW/m^2 was obtained from acetate in thermophilic MFCs using pure cultures (Fu et al., 2013b; Marshall and May, 2009; Sekar et al., 2017) or higher substrate concentrations (Fu et al., 2013b; Mathis et al., 2008).

248 Power peaks over 0.20 W/m^3 were obtained at the beginning of each feeding cycle, but then power
249 production decreased over time due to acetate and catholyte depletion (Fig. 1). This was attributed
250 to the highly capacitive activated carbon granules of the up-flow MFC, which accumulated
251 electrons (Deeke et al., 2015) when the catholyte was depleted, and quickly released them when
252 fresh catholyte was provided, resulting in the observed voltage peaks. Over the entire up-flow MFC
253 operation, with the exception of the first 2-3 d of each feeding cycle, the acetate consumption was
254 linear, suggesting first order kinetics with an average acetate removal rate of 68.6±17.1 mg/L/d. The
255 pH of the anolyte was relatively stable, ranging between 6.7 and 7.0, over the 202 d of operation.
256 The results suggest that reproducible substrate degradation and power production can be achieved
257 with long-term operation of thermophilic, acetate-fed, up-flow MFCs.
258
259 During the up-flow MFC operation, the anodic potential ranged between 0 and 0.2 V, being higher
260 after the addition of fresh catholyte and then constantly decreasing (Fig. 1). Since the acetate
261 concentration decreased during the batch cycle, anodic potential would be expected to increase,
262 rather fall, over time according to the Nernst equation (Logan et al., 2006). However, the fast drop
263 of the cathodic potential, decreasing from 0.2 to below 0.1 during the batch cycle (Fig. 1), likely
264 triggered an anodic potential drop. Nevertheless, it should be noted that the cathode potential,
265 measured against the reference electrode at the anode, may be inaccurate due to the potential losses
266 caused by the AEM and the electrolyte.
267
268 On day 109, replacing 100% of the anolyte with fresh medium did not affect the power production
269 and acetate consumption rate. This suggests that anode-attached microorganisms were mainly
270 responsible for acetate consumption and electron transfer to the anode (Marshall and May, 2009).
271 On day 187, catholyte depletion resulted in a drop of the cathodic potential from 0.10 to -0.08 V,
272 which also triggered a decrease of the anodic potential (Fig. 1) and resulted in an interruption in

power production. However, the MFC performance was restored upon replacement of the catholyte (Fig. 1).

The CE of 16.4±2.5% obtained in this study was similar to the one obtained by Dai et al. (2017) in an ethanol-fed MFC inoculated with digester sludge (20.5%), but lower than the CE of 80-90% previously obtained from acetate using mixed cultures under thermophilic conditions (Jong et al., 2006; Wrighton et al., 2008). Electron sinks such as methane or hydrogen were not detected in the gas bags during this study, suggesting a minor role of competing, non-electrogenic pathways. However, most likely, a share of electrons was consumed by reduction of ferricyanide ions flowing from the cathodic to the anodic chamber through the AEM (Pandit et al., 2011), and a share of acetate anions were lost by diffusion through the AEM (Kim et al., 2007), decreasing the overall CE. Kim et al. (2007) reported a diffusivity of acetate through AEM of 2.6×10^{-9} cm^2/s, which resulted in a 2.2% CE loss. In this study, the diffusivity of acetate was, in theory, substantially higher due to the higher temperature (55 °C *vs*. 30 °C) and membrane area (12.5 cm^2 for the upflow MFC and 22 cm^2 for the flow-through MFC *vs*. 3.5 cm^2) than the H-type MFC used by Kim et al. (2007). The same can be hypothesised for the diffusivity of ferricyanide, resulting in the relatively low CE obtained in this study.

Figure 1

3.2 Power production from acetate in the flow-through MFC

The flow-through MFC was inoculated with 10 mL anolyte from the up-flow MFC to evaluate the impact of the MFC configuration on the microbial community and power production, whilst keeping the operating parameters, such as temperature, pH and recirculation flow, similar. Anode electrode and hydrodynamic conditions were the main differences between the up-flow and the

298 flow-through MFC. The up-flow MFC anode had a higher total surface (94 cm^2, anode:membrane
299 ratio 7.5) than the flow-through MFC (22 cm^2, anode:membrane ratio 1.0). Furthermore, the
300 activated carbon granules of the up-flow MFC anode electrode were characterised by a high specific
301 surface (500-2000 m^2/g) (Mohan and Singh, 2005), providing more available surface than the
302 carbon paper electrode of the flow-through MFC for microbial adhesion. Hydrodynamically, the up-
303 flow MFC had a vertical flow with an up-flow velocity of 1.3 m/h, whereas the flow-through MFC
304 had a horizontal flow velocity of 12 m/h, although the same recirculation flow of 60 mL/min was
305 applied to the two MFCs, due to the different section area of the anodic chambers.
306
307 The power production onset occurred after only two days of flow-through MFC operation, and then
308 the power density increased peaking at 0.13 W/m^3 on day 6 (Fig. 2). This suggests that the
309 planktonic community from the up-flow MFC can be used as inoculum for other MFCs without
310 further BESA addition and start-up with an applied potential. Indeed, the anodic potential decreased
311 from the initial value of 0.26 V to -0.02 V on day 15, suggesting the development of the
312 electrogenic microbial community, but then increased again and stabilised to approximately 0.09 V
313 on days 30-45 (Fig. 2). Power peaks of 0.16-0.19 W/m^3 were observed after addition of fresh
314 anolyte and catholyte (on days 15 and 36), or just catholyte (on days 21 and 28), but power
315 production then decreased to <0.13 W/m^3 within two days. Lower anodic potential shifts were
316 obtained in the flow-through MFC, in comparison to the up-flow MFC, upon catholyte replacement
317 likely due to the different anode electrode material.
318
319 During the second and third feeding cycles, the average power density, CE and acetate consumption
320 rate were 0.11±0.1 W/m^3 (25.1±2.4 mW/m^2), 18.4±0.8%, and 54.5±5.1 mg/L/d, respectively (Table
321 1). Notwithstanding the different MFC designs, no statistically significant difference (p=0.05) was
322 observed between the up-flow and flow-through MFCs with respect to the average power

production per anolyte volume, CE, or acetate consumption rate (Table 1). This suggests that the MFC design had a minimum impact on the performance, although the average power normalised to the anode electrode surface was higher in the flow-through MFC than in the up-flow MFC (Table 1) due to the smaller electrode surface.

Figure 2

Table 1

3.3 Polarisation analyses of the up-flow and flow-through MFC

A maximum power production per anolyte volume of 0.22 W/m^3 and 0.11 W/m^3 was obtained in the up-flow and in the flow-through MFC with an external load of 250 and 100 Ω, respectively (Fig. 3). It is worth mentioning that, in the flow-through MFC, a higher power density (0.17 W/m^3) was obtained on day 17 before disconnecting the electrodes for the polarisation analysis (Fig. 2), compared to 0.11 W/m^3 obtained when the same resistance (100 Ω) was applied during polarisation (Fig. 3). The abrupt anodic potential changes due to the resistance changes during polarisation analysis may have affected the electroactive community, but power production increased again to 0.14 W/m^3 within two days after connecting the electrodes through the 100 Ω resistor (Fig. 2). The same phenomenon was not observed in the up-flow MFC, likely due to the presence of a more mature electroactive biofilm, resilient to potential changes, on the anode electrode when the polarisation analysis was performed on day 45. The maximum power normalised to the anode electrode surface was 11.6 and 24.2 mW/m^2 for the up-flow and flow-through MFC, respectively. The internal resistance of both the up-flow and flow-through MFC was around 160-180 Ω. However, the different shape of the polarisation curve (Fig. 3) suggests that ohmic losses were the prevalent cause of overpotential in the up-flow MFC, whereas activation losses were also important in the flow-through MFC (Logan et al., 2006).

Figure 3

3.4 Microbial communities in the up-flow and flow-through MFCs

The microbial communities populating the up-flow and flow-through MFCs were analysed at the level of both DNA and RNA to reveal the composition of the whole microbial community and the active portion, respectively. Alpha diversity analysis (Fig. 4) indicated significant differences in the microbial community composition between reactor (up-flow and flow-through MFC), and between DNA and RNA profiles. This was further supported by NMDS analysis (Fig. 4), which revealed distinct clustering based on MFC configuration, and between DNA and RNA profiles (PERMANOVA: P=0.001). Overall, communities appeared to cluster more closely based on reactor type, rather than nucleic acid, indicating that configuration and sample site (attached or planktonic) have a large influence on community composition. Clear separation was observed between the flow-through inoculum (up-flow planktonic community) and its final state (flow-through planktonic community) after 45 days of operation indicating that the MFC configuration severely affected the microbial community dynamics.

The total, and active, microbial community found in the up-flow MFC was highly diverse, particularly in the anodic biofilm where the Shannon diversity index was >2 (Fig. 4). The species richness, community evenness and the diversity were significantly lower in the planktonic community sampled after 45 days of operation of the flow-through MFC than in the planktonic community from the up-flow MFC, used as the inoculum. This indicates the evolution of a specialised community in the flow-through MFC, dominated by a small number of key species (Fig. 4), with a less even distribution than the community developed in the up-flow MFC. The low microbial diversity can be attributed to the more severe hydrodynamic conditions of the flow-

374 through than the up-flow MFC, which selected the species able to survive, and possibly transfer
375 electrons to the anode electrode, despite the high flow velocity (12 m/h). In particular, the shear
376 forces generated by the high recirculation flow, perpendicular to the anode electrode, strongly
377 affected biofilm formation, as suggested by the low nucleic acid concentration obtained in the
378 carbon paper samples. Furthermore, the species richness of the total (DNA-based) and active
379 (RNA-based) planktonic populations of the flow-through MFC was not significantly different, thus
380 indicating that most of the community present was active. This suggests that, based on very little
381 redundancy, the MFC may be vulnerable to environmental changes (Carballa et al., 2015, 2011).
382 Conversely, redundant microorganisms were present in the up-flow configuration MFC, as
383 suggested by the lower species richness at RNA than DNA level in both the attached and planktonic
384 communities.
385
386 **Figure 4**
387
388 *Tepidiphilus* sp. was the most abundant genus in the up-flow MFC, with a relative abundance of 30-
389 40% in anode-attached biofilm communities and 50-60% in planktonic communities based on both
390 DNA and cDNA sequences (Fig. 5). The *Tepidiphilus* genus belongs to the family of
391 *Hydrogenophilaceae*, which mostly includes chemolithotrophic microorganisms using hydrogen, or
392 inorganic sulfur compounds, as electron donor. However, it represents an exception, as it can grow
393 heterotrophically on a variety of substrates, including acetate (Manaia et al., 2003). Known isolates
394 of *Tepidiphilus* sp. is motile with a single, polar flagellum (Manaia et al., 2003; Poddar et al., 2014),
395 which could explain its high relative abundance among the planktonic community of the up-flow
396 MFC (Fig. 5). Its relative abundance of 30.5±0.9% in the transcriptionally-active portion of the
397 attached biofilm community suggests its ability to grow also on the anode. *Tepidiphilus* sp. was the
398 most abundant genus at DNA level (62±3%), but not at RNA level (34±2%), among the planktonic

community of the flow-through MFC (Fig. 5), suggesting the reduced importance of this microorganism when transferred from the up-flow to the flow-through MFC, and/or, indeed, an increase of the relative abundance of other members of the community (Fig. 5).

Coprothermobacter sp. was the second most abundant (20%) planktonic microorganism in the up-flow MFC and was previously found in several thermophilic environments, including bioelectrochemical systems (Dessì et al., 2018; Fu et al., 2013c; Jong et al., 2006; Sasaki et al., 2013). However, its electrogenic activity has not yet been confirmed in pure culture studies. *Coprothermobacter* sp. is strictly anaerobic, proteolytic, hydrogen-producing organisms, capable of hydrogen production via acetate oxidation (Gagliano et al., 2015), known to form growth-promoting syntrophic interactions with methanogens in anaerobic digesters (Sasaki et al., 2011). Dai et al. (2017) reported a significant reduction in relative abundance of *Coprothermobacter* sp. along with methanogens after dosing BESA to a thermophilic MFC. However, in this study, *Coprothermobacter* sp. remained among the most abundant species in the entire, and transcriptionally-active, communities upon elimination of methanogens with BESA, suggesting that another syntrophic interaction was formed, where the hydrogen produced by *Coprothermobacter* sp. facilitated interspecies electron transfer with another organism, or, perhaps, even directly to the anode electrode. The relative abundance of *Coprothermobacter* sp. decreased to below 2% in the active (and total) microbial community after 45 days of flow-through MFC operation (Fig. 5), suggesting a much smaller role for the microorganism in the flow-through than in the up-flow MFC. This coincided with relatively fewer *Tepidiphilus* sp. in the active community, indicating that *Tepidiphilus* sp. might indeed have been its syntrophic partner. However, testing that hypothesis will require further ecophysiological and culturing studies.

In the up-flow MFC, the relative abundance of *Ureibacillus* sp. was approximately 20% in the whole, and active, biofilm community, but it was relatively rare (1%) in the planktonic community (Fig. 5). Inoculation of the flow-through MFC with the planktonic community from the up-flow MFC favoured the establishment of *Ureibacillus* sp., which became the most abundant (>60%) active microorganism in the planktonic community after 45 days of flow-through MFC operation (Fig. 5). The relative abundance of *Ureibacillus* sp. appeared even higher (>90%) among the biofilm community of the flow-through MFC (Fig. 5), although no statistically significant analysis was performed using this sample as insufficient replicates were available. *Ureibacillus* sp. is a gram-negative microorganism, with an optimum growth temperature of 55°C, and can use acetate as substrate (Zhou et al., 2014). Despite being generally aerobic, *Ureibacillus* sp. was previously isolated from the anodic biofilm of a thermophilic MFC fed with sewage sludge (Zhou et al., 2014), suggesting its tolerance to anaerobic conditions. *Ureibacillus* sp. was shown to produce respiratory quinones possibly involved in mediated electron transfer to the electrode (Newman and Kolter, 2000), which would explain its high abundance in planktonic form in the flow-through MFC (Fig. 5), and the power production obtained despite the low biofilm formation.

The growth of *Ureibacillus* sp. in the flow-through MFC was accompanied by relatively increasingly abundant *Symbiobacterium* sp., which was outside the top-20 OTUs in the up-flow MFC but the third-most abundant taxa in the flow-through MFC (Fig. 5). *Symbiobacterium* sp. is a moderately anaerobic microorganism previously found in a thermophilic ethanol-fed MFC (Dai et al., 2017), indicating its possible involvement in thermophilic electricity production. *Symbiobacterium* sp. is unable to grow independently in any artificial medium, but was grown in co-culture (e.g., with *Bacillus* sp.) (Ohno et al., 2000). This suggests that its increased relative abundance in the flow-through MFC can be linked to the prevalence of *Ureibacillus* sp. (Fig. 5).

448 **Figure 5**

449

450 *3.5 Implications of the results and perspectives*

451 Despite being, in theory, thermodynamically and kinetically superior than the mesophilic MFCs, the
452 use of thermophilic MFCs is currently limited to fundamental research, using basic, H-type devices,
453 and there is a lack of information on the thermophilic, electrogenic microorganisms. Increasing the
454 technological level of thermophilic MFCs, as well as expanding the database of thermophilic
455 microorganisms colonizing the anode electrodes and anodic chamber, is now required to bridge the
456 gap with the more advanced mesophilic MFCs. This study investigates, for the first time, the
457 performance of two different MFC configurations, i.e. up-flow and flow-through MFCs, for
458 electricity production under thermophilic conditions. Further research is necessary on MFC design
459 and materials, as previously done for mesophilic MFCs, to increase power generation in
460 thermophilic MFCs.

461

462 The microbial community analysis, performed at both DNA and RNA level, showed a clear
463 difference between the microbial communities developing in the two MFC, but this had a minimum
464 impact on power production. This suggest that the different hydrodynamic conditions of up-flow
465 and flow-through MFCs impact the electrogenic consortia, but this not necessarily affects power
466 production. The results show that thermophilic microorganisms such as *Tepidiphilus* sp.,
467 *Ureibacillus* sp., and *Coprothermobacter* sp. are potentially electrogenic, but their potential for
468 electricity production in MFCs must be evaluated in pure culture studies.

469

470 **4. Conclusions**

471 An up-flow and a flow-through MFC were investigated, for the first time, for electricity production
472 from acetate under thermophilic conditions (55°C). *Tepidiphilus* sp. and *Ureibacillus* sp. were the

most abundant active microorganisms in the up-flow and flow-through MFC, respectively, suggesting their involvement in electricity production at 55°C. However, the similar power density (0.11-0.13 W/m^3), acetate degradation rate (55-69 mg/L/d) and coulombic efficiency (16-18%) of the two MFCs suggests there was a minimum impact of the microbial community composition on the overall MFC performance. Thermophilic microbial electrogenic consortia are thus resilient and canable to adapt to different MFC configurations.

Supplementary material

E-supplementary data for this work can be found in e-version of this paper online.

Acknowledgements

This work was supported by the Marie Skłodowska-Curie European Joint Doctorate (EJD) in Advanced Biological Waste-To-Energy Technologies (ABWET) funded from Horizon 2020 under grant agreement no. 643071 and the Science Foundation of Ireland (SFI) Research Professorship Programme (award no. 15/RP/2763). GC was supported by a Science Foundation Ireland Career Development Award (17/CDA/4658).

References

APHA, 1998. Standard Methods for the Examination of Water and Wastewater, twentieth ed. American Public Health Association/American Water Works Association/Water Environment Federation, Washington DC.

Caporaso, J.G., Lauber, C.L., Walters, W.A., Berg-Lyons, D., Lozupone, C.A., Turnbaugh, P.J., Fierer, N., Knight, R., 2011. Global patterns of 16S rRNA diversity at a depth of millions of sequences per sample. Proc. Natl. Acad. Sci. U. S. A. 108, 4516–22. https://doi.org/10.1073/pnas.1000080107

Carballa, M., Regueiro, L., Lema, J.M., 2015. Microbial management of anaerobic digestion: Exploiting the microbiome-functionality nexus. Curr. Opin. Biotechnol. 33, 103–111. https://doi.org/10.1016/j.copbio.2015.01.008

Carballa, M., Smits, M., Etchebehere, C., Boon, N., Verstraete, W., 2011. Correlations between molecular and operational parameters in continuous lab-scale anaerobic reactors. Appl. Microbiol. Biotechnol. 89, 303–314. https://doi.org/10.1007/s00253-010-2858-y

Carver, S.M., Vuoriranta, P., Tuovinen, O.H., 2011. A thermophilic microbial fuel cell design. J. Power Sources 196, 3757–3760. https://doi.org/10.1016/j.jpowsour.2010.12.088

Cecconet, D., Bolognesi, S., Molognoni, D., Callegari, A., Capodaglio, A.G., 2018. Influence of reactor's hydrodynamics on the performance of microbial fuel cells. J. Water Process Eng. 26, 281–288. https://doi.org/10.1016/j.jwpe.2018.10.019

Dai, K., Wen, J.L., Zhang, F., Ma, X.W., Cui, X.Y., Zhang, Q., Zhao, T.J., Zeng, R.J., 2017. Electricity production and microbial characterization of thermophilic microbial fuel cells. Bioresour. Technol. 243, 512–519. https://doi.org/10.1016/j.biortech.2017.06.167

Dattatraya Saratale, G., Ganesh Saratale, R., Kashif Shadid, M., Zhen, G., Kumar, G., Shin, H.-S., Choi, Y.-G., Kim, S.-H., 2017. A comprehensive overview on electro-active biofilms , role of exo-electrogens and their microbial niches in microbial fuel cells (MFCs). Chemosphere 178, 534–547. https://doi.org/10.1016/j.chemosphere.2017.03.066

Deeke, A., Sleutels, T.H.J.A., Donkers, T.F.W., Hamelers, H.V.M., Buisman, C.J.N., Ter Heijne, A., 2015. Fluidized capacitive bioanode as a novel reactor concept for the microbial fuel cell. Environ. Sci. Technol. 49, 1929–1935. https://doi.org/10.1021/es503063n

Dessì, P., Porca, E., Haavisto, J., Lakaniemi, A.-M., Collins, G., Lens, P.N.L., 2018. Composition and role of the attached and planktonic active microbial communities in mesophilic and thermophilic xylose-fed microbial fuel cells. RSC Adv. 8, 3069–3080. https://doi.org/10.1039/c7ra12316g

523 Dopson, M., Ni, G., Sleutels, T.H.J.A., 2016. Possibilities for extremophilic microorganisms in
524 microbial electrochemical systems. FEMS Microbiol. Rev. 40, 164–181.
525 https://doi.org/10.1093/femsre/fuv044
526 Fu, Q., Fukushima, N., Maeda, H., Sato, K., Kobayashi, H., 2015. Bioelectrochemical analysis of a
527 hyperthermophilic microbial fuel cell generating electricity at temperatures above 80 °C. Biosci.
528 Biotechnol. Biochem. 79, 1200–1206. https://doi.org/10.1080/09168451.2015.1015952
529 Fu, Q., Kobayashi, H., Kawaguchi, H., Vilcaez, J., Wakayama, T., Maeda, H., Sato, K., 2013a.
530 Electrochemical and phylogenetic analyses of current-generating microorganisms in a
531 thermophilic microbial fuel cell. J. Biosci. Bioeng. 115, 268–271.
532 https://doi.org/10.1016/j.jbiosc.2012.10.007
533 Fu, Q., Kobayashi, H., Kawaguchi, H., Wakayama, T., Maeda, H., Sato, K., 2013b. A thermophilic
534 gram-negative nitrate-reducing bacterium, *Calditerrivibrio nitroreducens*, exhibiting electricity
535 generation capability. Environ. Sci. Technol. 47, 12583–12590.
536 https://doi.org/10.1021/es402749f
537 Fu, Q., Kobayashi, H., Kuramochi, Y., Xu, J., Wakayama, T., Maeda, H., Sato, K., 2013c.
538 Bioelectrochemical analyses of a thermophilic biocathode catalyzing sustainable hydrogen
539 production. Int. J. Hydrogen Energy 38, 15638–15645.
540 https://doi.org/10.1016/j.ijhydene.2013.04.116
541 Gagliano, M.C., Braguglia, C.M., Petruccioli, M., Rossetti, S., 2015. Ecology and biotechnological
542 potential of the thermophilic fermentative *Coprothermobacter* spp. FEMS Microbiol. Ecol. 91,
543 5. https://doi.org/10.1093/femsec/fiv018
544 Griffiths, R.I., Whiteley, A.S., O'Donnell, A.G., Bailey, M.J., 2000. Rapid method for coextraction
545 of DNA and RNA from natural environments for analysis of ribosomal DNA- and rRNA-based
546 microbial community composition. Appl. Environ. Microbiol. 66, 5488–5491.
547 https://doi.org/10.1128/AEM.66.12.5488-5491.2000

548 Ha, P.T., Lee, T.K., Rittmann, B.E., Park, J., Chang, I.S., 2012. Treatment of alcohol distillery
549 wastewater using a bacteroidetes-dominant thermophilic microbial fuel cell. Environ. Sci.
550 Technol. 46, 3022–3030. https://doi.org/10.1021/es203861v
551 Haavisto, J., Dessì, P., Chatterjee, P., Honkanen, M., Noori, T., Kokko, M., Lakaniemi, A.-M., Lens,
552 P.N.L., Puhakka, J.A., 2019. Effects of anode materials on electricity production from xylose
553 and treatability of TMP wastewater in an up-flow microbial fuel cell. Chem. Eng. J. 372, 141–
554 150. https://doi.org/10.1016/j.cej.2019.04.090
555 Haavisto, J.M., Kokko, M.E., Lay, C.-H., Puhakka, J.A., 2017. Effect of hydraulic retention time on
556 continuous electricity production from xylose in up-flow microbial fuel cell. Int. J. Hydrogen
557 Energy 42, 27494–27501. https://doi.org/10.1016/j.ijhydene.2017.05.068
558 Jong, B.C., Kim, B.H., Chang, I.S., Liew, P.W.Y., Choo, Y.F., Kang, G.S., 2006. Enrichment,
559 performance, and microbial diversity of a thermophilic mediatorless microbial fuel cell. Environ.
560 Sci. Technol. 40, 6449–6454.
561 Kim, J.R., Cheng, S., Oh, S.-E., Logan, B.E., 2007. Power generation using different cation, anion,
562 and ultrafiltration membranes in microbial fuel cells. Environ. Sci. Technol. 41, 1004–1009.
563 https://doi.org/10.1021/es062202m
564 Kumar, A., Hsu, L.H.-H., Kavanagh, P., Barrière, F., Lens, P.N.L., Lapinsonnière, L., Lienhard V,
565 J.H., Schröder, U., Jiang, X., Leech, D., 2017. The ins and outs of microorganism–electrode
566 electron transfer reactions. Nat. Rev. Chem. 1, 24. https://doi.org/10.1038/s41570-017-0024
567 Lay, C.H., Kokko, M.E., Puhakka, J.A., 2015. Power generation in fed-batch and continuous up-flow
568 microbial fuel cell from synthetic wastewater. Energy 91, 235–241.
569 https://doi.org/10.1016/j.energy.2015.08.029
570 Logan, B.E., Hamelers, B., Rozendal, R., Schröder, U., Keller, J., Freguia, S., Aelterman, P.,
571 Verstraete, W., Rabaey, K., 2006. Microbial fuel cells: Methodology and technology. Environ.
572 Sci. Technol. 40, 5181–5192. https://doi.org/10.1021/es0605016

573 Lusk, B.G., Khan, Q.F., Parameswaran, P., Hameed, A., Ali, N., Rittmann, B.E., Torres, C.I., 2015.
574 Characterization of electrical current-generation capabilities from thermophilic bacterium
575 *Thermoanaerobacter pseudethanolicus* using xylose, glucose, cellobiose, or acetate with fixed
576 anode potentials. Environ. Sci. Technol. 49, 14725–14731.
577 https://doi.org/10.1021/acs.est.5b04036
578 Mäkinen, A.E., Nissilä, M.E., Puhakka, J.A., 2012. Dark fermentative hydrogen production from
579 xylose by a hot spring enrichment culture. Int. J. Hydrogen Energy 37, 12234–12240.
580 https://doi.org/10.1016/j.ijhydene.2012.05.158
581 Manaia, C., Nogales, B., Nunes, O.C., 2003. *Tepidiphilus margaritifer* gen. nov., sp. nov., isolated
582 from a thermophilic aerobic digester. Int. J. Syst. Evol. Microbiol. 53, 1405–1410.
583 https://doi.org/10.1099/ijs.0.02538-0
584 Marshall, C.W., May, H.D., 2009. Electrochemical evidence of direct electrode reduction by a
585 thermophilic Gram-positive bacterium, *Thermincola ferriacetica*. Energy Environ. Sci. 2, 699–
586 705. https://doi.org/10.1039/B823237G
587 Mathis, B.J., Marshall, C.W., Milliken, C.E., Makkar, R.S., Creager, H.D., May, H.D., 2008.
588 Electricity generation by thermophilic microorganisms from marine sediment. Appl. Microbiol.
589 Biotechnol. 78, 147–155. https://doi.org/10.1007/s00253-007-1266-4
590 Mohan, D., Singh, K., 2005. Granular activated carbon. Water encyclopedia (eds. J. H. Lehr and J.
591 Keeley).
592 Newman, D.K., Kolter, R., 2000. A role for excreted quinones in extracellular electron transfer.
593 Nature 405, 94–97. https://doi.org/10.1038/35011098
594 Ohno, M., Shiratori, H., Park, M.-J., Saitoh, Y., Kumon, Y., Yamashita, N., Hirata, A., Nishida, H.,
595 Ueda, K., Beppu, T., 2000. *Symbiobacterium thermophilum* gen. nov., sp. nov., a symbiotic
596 thermophile that depends on co-culture with a *Bacillus* strain for growth. Int. J. Syst. Evol.
597 Microbiol. 50, 1829–1832.

598 Oksanen, J., Blanchet, F., Kindt, R., Legendre, P., Minchin, P., O'hara, R, et al., 2015. Vegan:
599 community ecology package. R Packag. version 2.2-1.
600 Pandit, S., Sengupta, A., Kale, S., Das, D., 2011. Performance of electron acceptors in catholyte of a
601 two-chambered microbial fuel cell using anion exchange membrane. Bioresour. Technol. 102,
602 2736–2744. https://doi.org/10.1016/j.biortech.2010.11.038
603 Parameswaran, P., Bry, T., Popat, S.C., Lusk, B.G., Rittmann, B.E., Torres, C.I., 2013. Kinetic,
604 electrochemical, and microscopic characterization of the thermophilic, anode-respiring
605 bacterium *Thermincola ferriacetica*. Environ. Sci. Technol. 47, 4934–4940.
606 https://doi.org/10.1021/es400321c
607 Poddar, A., Lepcha, R.T., Das, S.K., 2014. Taxonomic study of the genus Tepidiphilus: transfer of
608 Petrobacter succinatimandens to the genus Tepidiphilus as Tepidiphilus succinatimandens
609 comb. nov., emended description of the genus Tepidiphilus and description of. Int. J. Syst. Evol.
610 Microbiol. 64, 228–235. https://doi.org/10.1099/ijs.0.056424-0
611 Sasaki, D., Sasaki, K., Watanabe, A., Morita, M., Matsumoto, N., Igarashi, Y., Ohmura, N., 2013.
612 Operation of a cylindrical bioelectrochemical reactor containing carbon fiber fabric for efficient
613 methane fermentation from thickened sewage sludge. Bioresour. Technol. 129, 366–373.
614 https://doi.org/10.1016/j.biortech.2012.11.048
615 Sasaki, K., Morita, M., Sasaki, D., Nagaoka, J., Matsumoto, N., Ohmura, N., Shinozaki, H., 2011.
616 Syntrophic degradation of proteinaceous materials by the thermophilic strains
617 *Coprothermobacter proteolyticus* and *Methanothermobacter thermautotrophicus*. J. Biosci.
618 Bioeng. 112, 469–472. https://doi.org/10.1016/j.jbiosc.2011.07.003
619 Schloss, P.D., Westcott, S.L., Ryabin, T., Hall, J.R., Hartmann, M., Hollister, E.B., Lesniewski, R.A.,
620 Oakley, B.B., Parks, D.H., Robinson, C.J., Sahl, J.W., Stres, B., Thallinger, G.G., Van Horn,
621 D.J., Weber, C.F., 2009. Introducing mothur: Open-source, platform-independent, community-
622 supported software for describing and comparing microbial communities. Appl. Environ.

623 Microbiol. 75, 7537–7541. https://doi.org/10.1128/AEM.01541-09
624 Sekar, N., Wu, C.H., Adams, M.W.W., Ramasamy, R.P., 2017. Electricity generation by *Pyrococcus*
625 *furiosus* in microbial fuel cells operated at 90°C. Biotechnol. Bioeng. 114, 1419–1427.
626 https://doi.org/10.1002/bit.26271
627 Shrestha, N., Chilkoor, G., Vemuri, B., Rathinam, N., Sani, R.K., Gadhamshetty, V., 2018.
628 Extremophiles for microbial-electrochemistry applications: A critical review. Bioresour.
629 Technol. 255, 318–330. https://doi.org/10.1016/j.biortech.2018.01.151
630 Sulonen, M.L.K., Kokko, M.E., Lakaniemi, A.M., Puhakka, J.A., 2015. Electricity generation from
631 tetrathionate in microbial fuel cells by acidophiles. J. Hazard. Mater. 284, 182–189.
632 https://doi.org/10.1016/j.jhazmat.2014.10.045
633 ter Heijne, A., Hamelers, H.V.M., Saakes, M., Buisman, C.J.N., 2008. Performance of non-porous
634 graphite and titanium-based anodes in microbial fuel cells. Electrochim. Acta 53, 5697–5703.
635 https://doi.org/10.1016/j.electacta.2008.03.032
636 Wrighton, K.C., Agbo, P., Warnecke, F., Weber, K.A., Brodie, E.L., DeSantis, T.Z., Hugenholtz, P.,
637 Andersen, G.L., Coates, J.D., 2008. A novel ecological role of the Firmicutes identified in
638 thermophilic microbial fuel cells. ISME J. 2, 1146–1156. https://doi.org/10.1038/ismej.2008.48
639 Wrighton, K.C., Thrash, J.C., Melnyk, R.A., Bigi, J.P., Byrne-Bailey, K.G., Remis, J.P., Schichnes,
640 D., Auer, M., Chang, C.J., Coates, J.D., 2011. Evidence for direct electron transfer by a Gram-
641 positive bacterium isolated from a microbial fuel cell. Appl. Environ. Microbiol. 77, 7633–7639.
642 https://doi.org/10.1128/AEM.05365-11
643 Yang, L., Yi, G., Hou, Y., Cheng, H., Luo, X., Pavlostathis, S.G., Luo, S., Wang, A., 2019. Building
644 electrode with three-dimensional macroporous interface from biocompatible polypyrrole and
645 conductive graphene nanosheets to achieve highly efficient microbial electrocatalysis. Biosens.
646 Bioelectron. 141, 111444. https://doi.org/10.1016/j.bios.2019.111444
647 Zhou, S., Tang, J., Qin, D., Lu, Q., Yang, G., 2014. *Ureibacillus defluvii* sp. nov., isolated from a

thermophilic microbial fuel cell. Int. J. Syst. Evol. Microbiol. 64, 1617–1621. https://doi.org/10.1099/ijs.0.056655-0

Figure captions

Fig. 1. Power density (a), anodic and cathodic potential (b), and acetate concentration profiles (c) obtained from the up-flow MFC over the final three feeding cycles (days 161-202).

Fig. 2. Power density (a), anodic potential (b) and acetate concentration profiles (c) obtained in the flow-through MFC during the 45 days operation. Data are missing on day 17 when the polarisation analysis was conducted.

Fig. 3. Power (a) and polarisation (b) curves, normalised to the anolyte volume, obtained from the up-flow and flow-through MFC on operation days 45 and 17, respectively.

Fig. 4. Box plots representing Pielou's evenness, rarefied richness and Shannon Entropy alpha diversity indices (a) from microbiological samples from the up-flow MFC (UMFC) or the flow-through MFC (FTMFC) from DNA and cDNA sequences. The attached community of the flow-through MFC was excluded from this analysis due to the lack of replicates. Lines of significance depict significant differences as follows: * ($p<0.05$), ** ($p<0.01$), or *** ($p<0.001$) based on ANOVA. Non-Metric Multidimensional Scaling (NMDS) using Bray-Curtis dissimilarity metric (b). Each point represents a sample community structure. Reactor (upflow or flow-through), and nucleic acid (DNA and RNA) types are depicted by colour, and ellipses are constructed at a 95% confidence interval.

672 **Fig. 5.** Taxa plot representing the community structure of the top-25 most abundant OTUs across all
673 reactor configurations (up-flow MFC, UMFC and flow-through MFC, FTMFC) and nucleic acid
674 (DNA and RNA) combinations. ‘Others’ denotes any OTUs not within the top-25.

675 **Tables**

676 **Table 1.** Average and maximum power and current production, acetate consumption rate, coulombic efficiency and dominant microorganism

677 obtained in the up-flow and flow-through MFC.

MFC configuration	Feeding cycles	Power density (W/m^3)		Power density (mW/m^2)		Current density (A/m^2)		Acetate consumption rate (mg/L/d)	Coulombic efficiency (%)	Dominant microorganism
		Average[b]	Peak[c]	Average	Peak	Average	Peak			
Up-flow	2-15[a]	0.13±0.03	0.28±0.06	8.4±2.2	14.7±3.4	0.09±0.01	0.12±0.01	68.6±17.1	16.4±2.5	*Tepidiphilus sp.*
Flow-through	2-3[a]	0.11±0.01	0.18±0.01	25.1±2.4	41.3±2.7	0.34±0.02	0.43±0.01	54.5±5.1	18.4±0.8	*Ureibacillus sp.*

678 [a] The first feeding cycle was considered start-up stage and excluded from the analysis

679 [b] Average calculated on the feeding cycles 2-15 (day 8-202) for the up-flow MFC and on feeding cycle 2-3 (day 15-45) for the flow-through MFC

680 [c] Average of the power/current peaks obtained in each feeding cycle

Figures

Figure 1

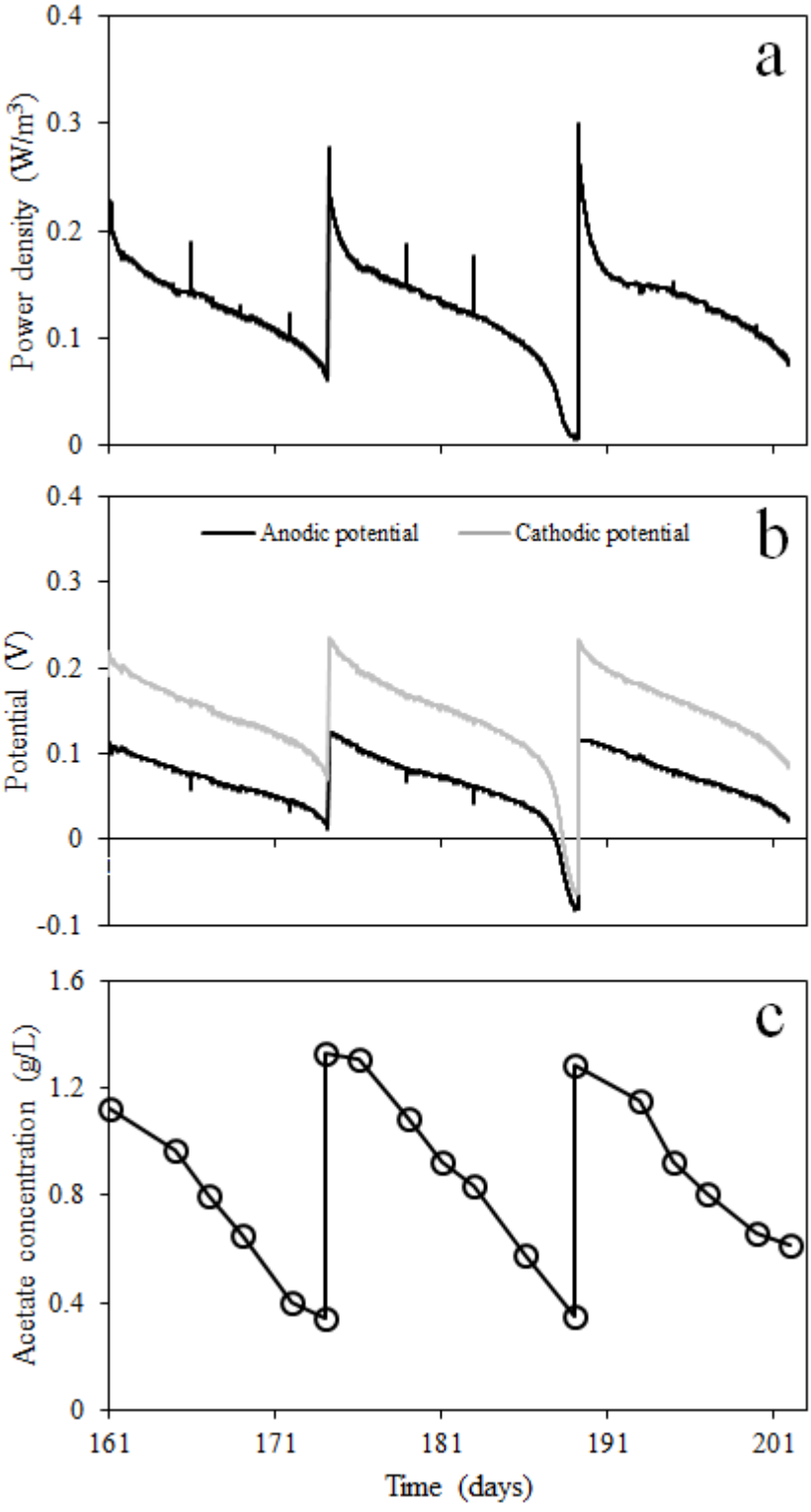

686 **Figure 2**

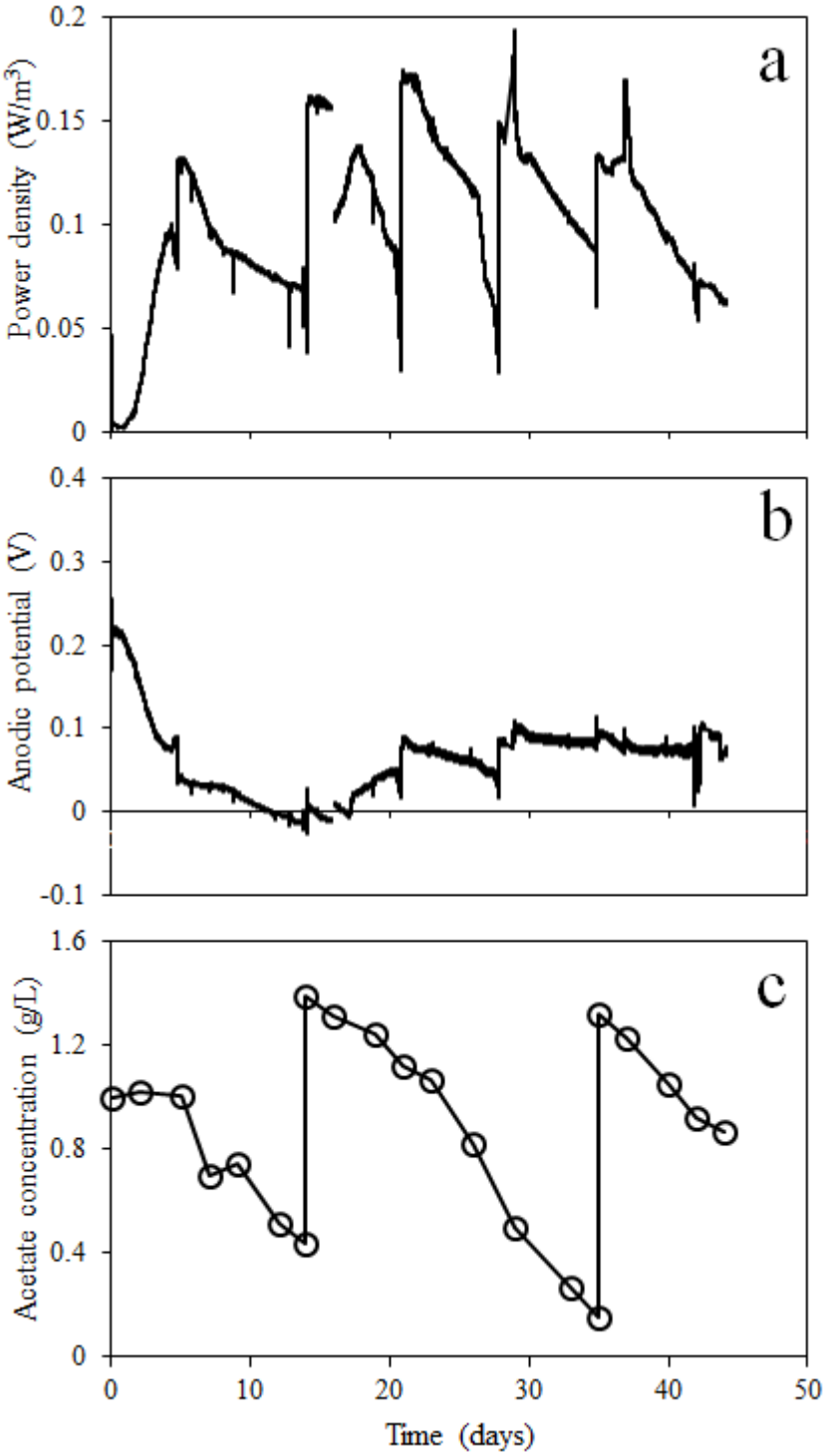

687

688

689

690

691

692 **Figure 3**

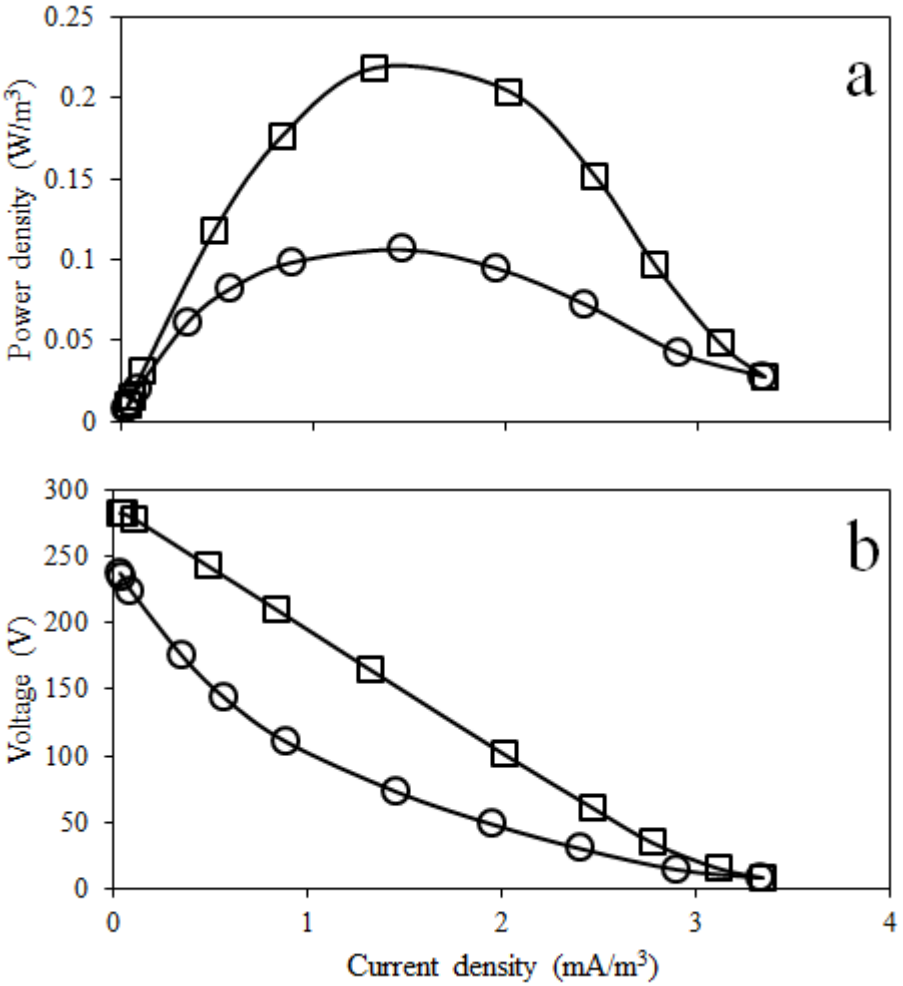

693

694

695

696

697

698

699

700

701

702

703

Figure 4

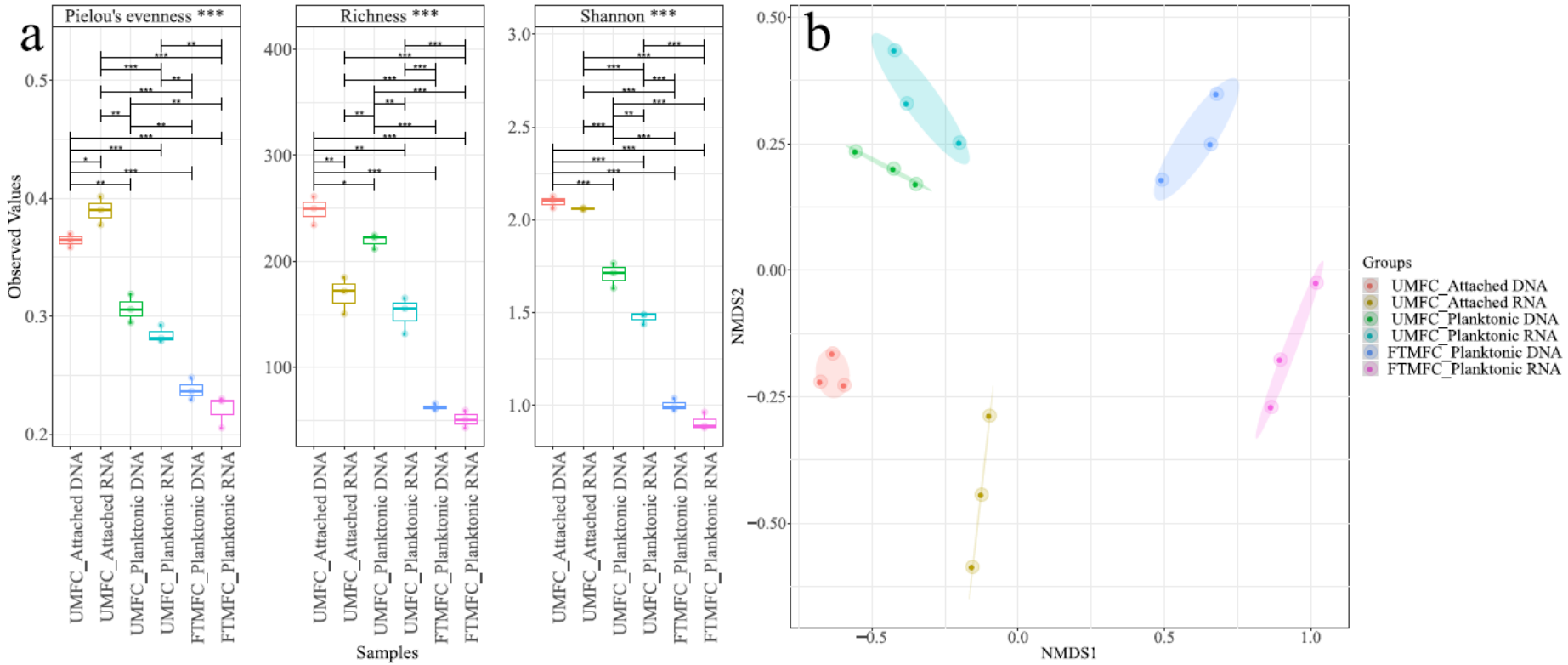
a
Pielou's evenness ***
Richness ***
Shannon ***
Observed Values
Samples
UMFC_Attached DNA
UMFC_Attached RNA
UMFC_Planktonic DNA
UMFC_Planktonic RNA
FTMFC_Planktonic DNA
FTMFC_Planktonic RNA
b
NMDS1
NMDS2
Groups
UMFC_Attached DNA
UMFC_Attached RNA
UMFC_Planktonic DNA
UMFC_Planktonic RNA
FTMFC_Planktonic DNA
FTMFC_Planktonic RNA

Figure 5

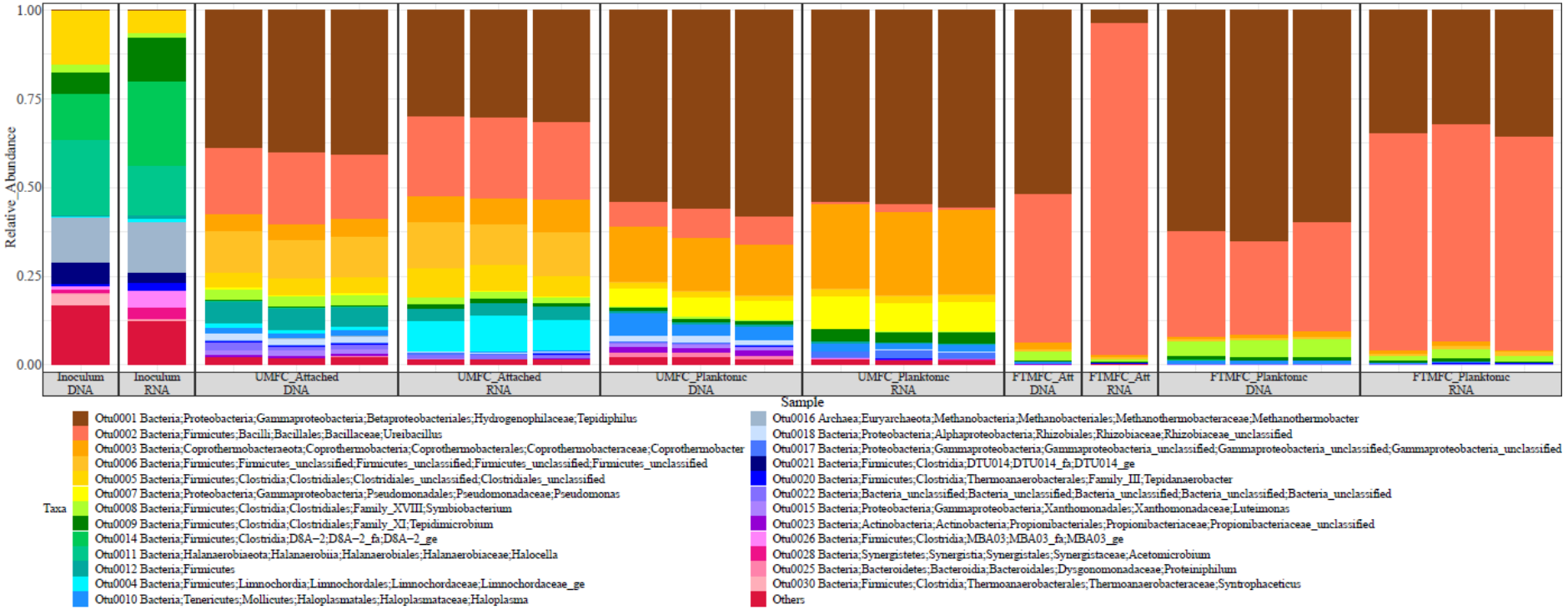
1.00
0.75
0.50
0.25
0.00
Relative Abundance
Inoculum DNA
Inoculum RNA
UMFC_Attached DNA
UMFC_Attached RNA
UMFC_Planktonic DNA
UMFC_Planktonic RNA
FTMFC_Att DNA
FTMFC_Att RNA
FTMFC_Planktonic DNA
FTMFC_Planktonic RNA
Sample
Taxa
Otu0001 Bacteria;Proteobacteria;Gammaproteobacteria;Betaproteobacteriales;Hydrogenophilaceae;Tepidiphilus
Otu0002 Bacteria;Firmicutes;Bacilli;Bacillales;Bacillaceae;Ureibacillus
Otu0003 Bacteria;Coprothermobacteraeota;Coprothermobacteria;Coprothermobacterales;Coprothermobacteraceae;Coprothermobacter
Otu0006 Bacteria;Firmicutes;Firmicutes_unclassified;Firmicutes_unclassified;Firmicutes_unclassified;Firmicutes_unclassified
Otu0005 Bacteria;Firmicutes;Clostridia;Clostridiales;Clostridiales_unclassified;Clostridiales_unclassified
Otu0007 Bacteria;Proteobacteria;Gammaproteobacteria;Pseudomonadales;Pseudomonadaceae;Pseudomonas
Otu0008 Bacteria;Firmicutes;Clostridia;Clostridiales;Family_XVIII;Symbiobacterium
Otu0009 Bacteria;Firmicutes;Clostridia;Clostridiales;Family_XI;Tepidimicrobium
Otu0014 Bacteria;Firmicutes;Clostridia;D8A−2;D8A−2_fa;D8A−2_ge
Otu0011 Bacteria;Halanaerobiaeota;Halanaerobiia;Halanaerobiales;Halanaerobiaceae;Halocella
Otu0012 Bacteria;Firmicutes
Otu0004 Bacteria;Firmicutes;Limnochordia;Limnochordales;Limnochordaceae;Limnochordaceae_ge
Otu0010 Bacteria;Tenericutes;Mollicutes;Haloplasmatales;Haloplasmataceae;Haloplasma
Otu0016 Archaea;Euryarchaeota;Methanobacteria;Methanobacteriales;Methanothermobacteraceae;Methanothermobacter
Otu0018 Bacteria;Proteobacteria;Alphaproteobacteria;Rhizobiales;Rhizobiaceae;Rhizobiaceae_unclassified
Otu0017 Bacteria;Proteobacteria;Gammaproteobacteria;Gammaproteobacteria_unclassified;Gammaproteobacteria_unclassified;Gammaproteobacteria_unclassified
Otu0021 Bacteria;Firmicutes;Clostridia;DTU014;DTU014_fa;DTU014_ge
Otu0020 Bacteria;Firmicutes;Clostridia;Thermoanaerobacterales;Family_III;Tepidanaerobacter
Otu0022 Bacteria;Bacteria_unclassified;Bacteria_unclassified;Bacteria_unclassified;Bacteria_unclassified
Otu0015 Bacteria;Proteobacteria;Gammaproteobacteria;Xanthomonadales;Xanthomonadaceae;Luteimonas
Otu0023 Bacteria;Actinobacteria;Actinobacteria;Propionibacteriales;Propionibacteriaceae;Propionibacteriaceae_unclassified
Otu0026 Bacteria;Firmicutes;Clostridia;MBA03;MBA03_fa;MBA03_ge
Otu0028 Bacteria;Synergistetes;Synergistia;Synergistales;Synergistaceae;Acetomicrobium
Otu0025 Bacteria;Bacteroidetes;Bacteroidia;Bacteroidales;Dysgonomonadaceae;Proteiniphilum
Otu0030 Bacteria;Firmicutes;Clostridia;Thermoanaerobacterales;Thermoanaerobacteraceae;Syntrophaceticus
Others

Power production and microbial community composition in thermophilic acetate-fed up-flow and flow-through microbial fuel cells

Paolo Dessì [a,b,*], *Pritha Chatterjee* [a,c], *Simon Mills*[d], *Marika Kokko*[a], *Aino-Maija Lakaniemi* [a], *Gavin Collins*[d], *Piet N. L. Lens*[a,b]

[a]*Tampere University, Faculty of Engineering and Natural Sciences, P.O. Box 541, FI- 33104 Tampere University, Finland*

[b]*National University of Ireland Galway, University Road, Galway, H91 TK33, Ireland*

[c]*Department of Civil Engineering, Indian Institute of Technology Hyderabad, India*

[d]*Microbial Communities Laboratory, School of Natural Sciences, National University of Ireland Galway, University Road, Galway, H91 TK33, Ireland*

Supplementary material

The file contains 1 Figure and 1 Table.

*****Corresponding author: Phone: +353 830678774, e-mail: paolo.dessi@nuigalway.ie

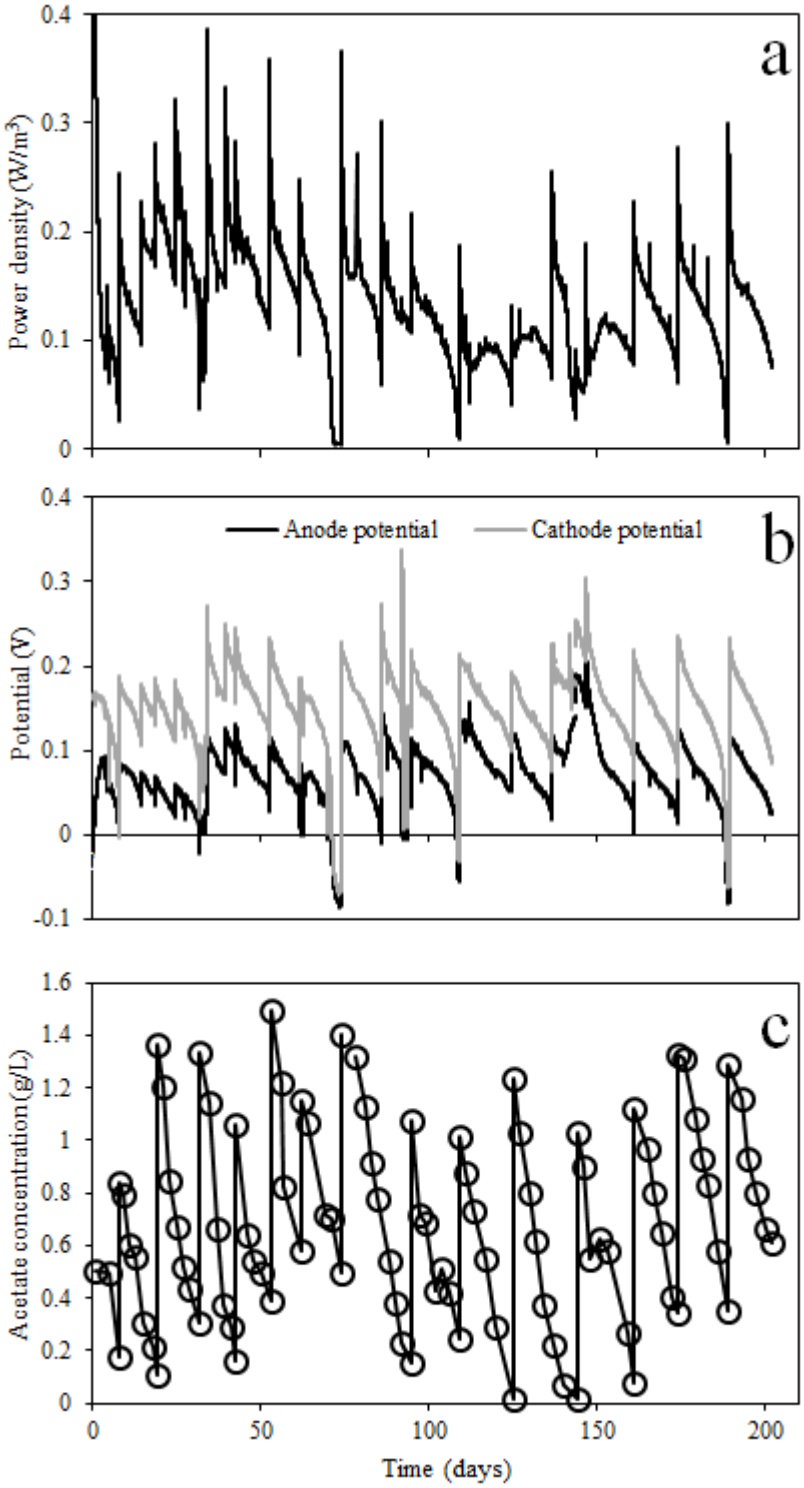

Fig. S1. Power density (a), anodic and cathodic potential (b) and acetate concentration profiles (c) obtained in the up-flow MFC in the 202 days of operation.

Table S1. Average and maximum power and current production, anodic and cathodic potential, acetate consumption rate and coulombic efficiency obtained in the up-flow MFC in the 15 fed-batch cycles and in the flow-through MFC in the 3 fed-batch cycles.

MFC configuration	Batch Cycle	Time period (days)	Power (W/m^3)		Power (mW/m^2)		Current (A/m^2)		Anodic potential (V)	Cathodic potential (V)	Acetate consumption rate (mg/L/d)	Coulombic efficiency (%)
			Average	Peak	Average	Peak	Average	Peak				
Up-flow	1	0 - 8	0.15	0.81	9.4	43.3	0.09	0.21	0.05	0.14	40.7	28.6
	2	8 - 19	0.15	0.25	9.6	13.5	0.09	0.12	0.07	0.15	66.9	17.6
	3	19 - 32	0.20	0.32	12.5	17.1	0.11	0.13	0.04	0.14	81.6	16.5
	4	32 - 43	0.18	0.39	11.1	20.5	0.10	0.15	0.08	0.18	108.2	11.7
	5	43 - 53	0.16	0.28	10.3	15.1	0.10	0.13	0.08	0.17	66.4	18.3
	6	53 - 62	0.17	0.36	10.9	19.1	0.10	0.14	0.08	0.17	102.1	12.3
	7	62 - 74	0.09	0.25	5.9	13.2	0.07	0.12	0.02	0.10	55.0	16.8
	8	74 - 95	0.15	0.37	9.3	19.5	0.09	0.14	0.08	0.16	59.8	19.3
	9	95 - 109	0.11	0.22	6.7	11.6	0.08	0.11	0.07	0.14	58.8	16.7
	10	109 - 125	0.09	0.19	5.5	9.9	0.07	0.10	0.09	0.16	62.7	14.2
	11	125 - 144	0.10	0.26	6.5	13.6	0.08	0.12	0.08	0.15	64.1	15.2
	12	144 - 161	0.09	0.19	5.9	10.0	0.07	0.10	0.10	0.17	56.0	16.5
	13	161 - 174	0.13	0.23	8.2	12.2	0.09	0.11	0.07	0.15	58.6	18.5
	14	174 - 189	0.12	0.26	7.3	13.8	0.08	0.12	0.06	0.14	65.2	15.8
	15	189 - 202	0.14	0.30	8.5	15.9	0.09	0.13	0.08	0.16	53.0	21.0
Flow-through	1	0 - 15	0.06	0.13	13.6	30.1	0.25	0.37	0.07	n.a.	37.7	19.6
	2	15 - 36	0.12	0.19	27.3	43.9	0.35	0.45	0.06	n.a.	59.6	17.6
	3	36 - 45	0.10	0.17	22.7	38.6	0.32	0.42	0.08	n.a.	49.5	19.2